

双核三螺旋铁配合物的合成和结构

郭 栋 李继辉 谢婧婧 段春迎* 孟庆金

(南京大学配位化学研究所, 配位化学国家重点实验室, 南京 210093)

本文选择了 2-羟基-1-萘醛与水合肼形成的席夫碱, $[(HO)(C_{10}H_6)CH=N-N=CH(C_{10}H_6)(OH)]$, 作为配体, 设计组装了双核三螺旋的三价铁配合物。配合物中每一个铁离子以准八面体的配位方式分别与三个 NO 双齿单元配位, 三个配体分别桥联两个金属形成特定的三螺旋构型。分子内和分子间的 $\pi-\pi$ 堆积作用对螺旋体的形成和堆积方式起着十分重要的作用。作为对照, 本文还报道了配体的晶体结构。

关键词: 三螺旋 席夫碱 晶体结构 分子堆积
分类号: O614.81+1

Synthesis and Crystal Structure of Triple-Helical Di-iron(III) Complex

GUO Dong LI Ji-Hui XIE Jing-Jing DUAN Chun-Ying* MENG Qing-Jin

(Coordination Chemistry Institute, The State Key Laboratory of Coordination Chemistry, Nanjing University, Nanjing 210093)

The self-assembly and structural characterization of the new iron(III) molecular helix Fe_2L_3 was achieved from an inexpensive and easy-to-prepare bis-bidentate Schiff base ligand, H_2L , $[(HO)(C_{10}H_6)CH=N-N=CH(C_{10}H_6)(OH)]$. The triple helical Fe_2L_3 molecule contains two iron(III) atoms and three ligands. Each metal center is bound to three bidentate NO units to attain a pseudo-octahedral co-ordination geometry. The ligand wraps in a helical arrangement around the two metal ions. It is suggested that the intramolecular and intermolecular $\pi-\pi$ stacking interactions play important roles in the metal-assisted self-assembling process. Crystal structure of the free ligand was also reported for comparison. CCDC: 197370, 197371.

Keywords: triple-helix schiff-base crystal structure molecular packing

0 Introduction

Within the field of supramolecular inorganic chemistry, self-assembly provides direct access to complex architectures comprising spatially and geometrically well defined arrays of metal ions^[1, 2]. The structure of the bridging group, the metal binding moiety, the metal coordination geometry as well as non-covalent interactions all dictate the architecture obtained. In

order to design species presenting special structural and functional features, it is of great importance to establish the rules by which the controlling of the self-assembly process can be achieved through chemical programming by means of suitable components and assembling algorithms^[3].

Helical complexes have elegantly illustrated how the formation of specific architecturally complex assemblies can be directed by the interplay between rel-

收稿日期: 2002-09-08。收修改稿日期: 2002-10-12。

国家自然科学基金资助项目(No. 20131020)。

* 通讯联系人。E-mail: duancy@nju.edu.cn

第一作者: 郭 栋, 男, 28 岁, 博士, 研究方向: 功能配位化学。

atively simple parameters, such as the stereoelectronic preference of the metal and the disposition of binding sites of helicands (helicate ligands)^[4]. A helicate is classically described as a discrete helical supramolecular complex composed of one or more covalent organic strands wrapped around a series of ions defining the helical axis. Many helicates are derived from ligands, which are obviously partitioned into two distinct bidentate binding sites and a spacer linking them together. For a dinuclear triple helical architecture, it is postulated^[5, 6] that a chosen spacer should firstly have enough rigidity that sterically prevents the two metal binding sites from coordinating to a single metal centre and secondly should introduce enough flexibility into the ligand backbone to permit the ligands to wrap around the metal-metal axis. Chiral helices will result only when the two metal ions display the same absolute configurations^[7, 8]. It is expected that the ligand used to build triple helicates only needs to be able to transmit the chirality from one metal center to another.

To establish our approach, ligand L with two NO bidentate sites connected by a single bond was chosen to address the challenge of creating triple-helical architectures. It should be noted that this is the shortest possible imine-based ligand system of this type^[9]. The rigidity of the ligand and the close proximity of the two metal centers seem unfavorable for triple helicate formation. A related system was reported by Ziessel, et. Al^[10], in which the two nitrogen donors were separated by a single carbon atom with a N...N separation of *ca.* 2.3 Å.

1 Experimental Section

1.1 Materials and Analyses

All chemicals were of reagent grade quality obtained from commercial sources and used without further purification. Elemental analyses (C, H and N) were carried out on a Perkin-Elmer 240 analyzer. IR spectra were recorded on a VECTOR 22 Bruker spectrophotometer with KBr pellets in the 4000 ~ 400 cm⁻¹ regions. Differential thermal analysis and thermogravimetric analysis (DTA-TGA) were conducted on a TA

instruments SDT 2960 simultaneous DTA-TGA in a nitrogen atmosphere at a heating rate of 5°C · min⁻¹.

1.2 Synthesis of the Free Ligand

To 50 mL methanol containing 2-hydroxy-1-naphthaldehyde (3.44 g, 20 mmol), hydrazine hydroxide (0.50 g, 10 mmol) was added. After refluxing for 4 h, yellow solid (H₂L) formed was isolated by filter and dried over P₂O₅ under vacuum. Yield: 84%. Anal. Calcd. for C₂₂H₁₆N₂O₄: C, 77.6; H, 4.7; N, 8.2. Found: C, 77.1; H, 5.0; N, 7.7. IR (cm⁻¹, KBr disk) 3251 (ν_{C-H}), 2852, 1619, 1589, 1514, 1465 (ν_{C=O}, ν_{C=N}), 1263 (ν_{N=N}).

1.3 Synthesis of the Dinuclear Triple Helix

To 25 mL methanol containing ligand H₂L (0.51 g, 1.5 mmol), Fe(NO₃)₃ · 9H₂O (0.41 g, 1 mmol) was added. After finishing the addition, the solution was stirred for 1 h at room temperature. Black solid was isolated by filter and dried over P₂O₅ under vacuum. Yield: 62%. Anal. Calcd for C₆₆H₄₂N₆O₁₂Fe₂: C, 66.9; H, 4.7; N, 9.4. Found: C, 67.7; H, 5.2; N, 9.7. Dark-red crystals suitable for X-ray structural determination were obtained by slow diffusion of diethyl ether into a DMF solution.

1.4 Crystallography

Parameters for data collection and refinement of complexes are summarized in Table 1. The intensities of the free ligand and the title complex were collected on a Siemens SMART-CCD diffractometer with graphite-monochromatic Mo Kα radiation (λ = 0.71073 Å) using SMART and SAINT program^[11]. The structures were solved by direct methods and refined on F² using full-matrix least-squares methods using SHELXTL version 5.1^[12]. Anisotropic thermal parameters were refined for non-hydrogen atoms. Hydrogen atoms were localized in their calculation positions and refined using riding model.

CCDC: 197370, 197371.

2 Results and Discussion

2.1 Synthesis and Crystal Structure of the Free Ligand

Ligand H₂L is prepared readily by simply mixing

Table 1 Crystallographic Data

empirical formula	C ₂₂ H ₁₆ N ₂ O ₂	[C ₂₂ H ₁₆ N ₂ O ₂] ₃ Fe ₂ (C ₃ H ₇ NO) ₃
formula weight	340.37	1346.07
temperature / K	293(2)	293(2)
wavelength / Å	0.71073	0.71073
crystal system	monoclinic	triclinic
space group	<i>P</i> 2(1)/ <i>n</i>	<i>P</i> $\bar{1}$
<i>a</i> / Å	13.82(2)	8.547(2)
<i>b</i> / Å	15.75(3)	6.109(2)
<i>c</i> / Å	16.02(2)	15.99(2)
α / (°)		98.40(3)
β / (°)	87.63(4)	87.63(4)
γ / (°)		67.63(3)
volume / Å ³	834.4	3218.9
<i>Z</i>	2	6
density (calculated) / (Mg · m ⁻³)	1.355	1.511
absorption coefficient / mm ⁻¹	0.088	0.744
<i>F</i> (000)	356	1512
reflections collected	4080	20407
independent reflections	1462 (<i>R</i> _m = 0.103)	14279 (<i>R</i> _m = 0.057)
goodness-of-fit on <i>F</i> ²	1.046	0.827
final <i>R</i> indices [<i>I</i> > 2σ(<i>I</i>)]	<i>R</i> ₁ = 0.048, <i>wR</i> ₂ = 0.138	<i>R</i> ₁ = 0.052, <i>wR</i> ₂ = 0.068
<i>R</i> indices (all data)	<i>R</i> ₁ = 0.052, <i>wR</i> ₂ = 0.148	<i>R</i> ₁ = 0.124, <i>wR</i> ₂ = 0.077
largest diff. peak and hole / (e · Å ⁻³)	0.225 and -0.218	0.472 and -0.285

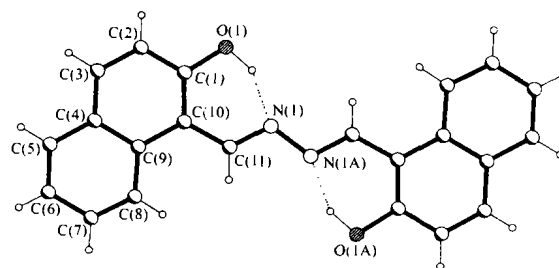
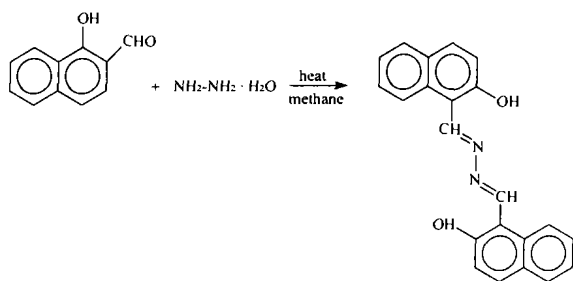


Fig. 1 Molecular structure of the free ligand with the atom numbering scheme

Symmetry code A: $2 - x, 1 - y, 2 - z$

Selected bond distances: N(1)-C(11), 1.285(2); N(1)-N(1A), 1.387(2); O(1)-C(1), 1.344(4); C(10)-C(11), 1.441(2) Å.

2-hydroxy-1-naphthaldehyde and hydrazine hydrate in methanol.

Molecule of ligand L (Fig. 1) is coplanar with the midpoint of the N-N bond lying across on an inversion center. The two nitrogen donors adopt a transoid configuration and in the presence of metal ions, molecules of ligand L are also able to function as a bis-(bidentate) ligand. However, it should be noted that such a strictly conjugated coplanar system seems unfavorable for triple helical formation. Bond distances of the Ar-CH=N-N=CH-Ar moiety are all intermediate between formal single and double bonds, pointing to extensive electron delocalization over the entire moiety. Classical O-H \cdots N hydrogen bonds between the OH groups and the imine nitrogen atoms were also found.

The O(1) \cdots N(1) separation is 2.570(6) Å and the angle of O(1W)-H(10) \cdots N(1) is 151°, respectively. Adjacent molecules of ligand L are organized into a one-dimensional chain by strong π - π stacking interactions of the aromatic rings in an offset fashion with a the shortest interplanar atom \cdots atom separation of ca. 3.31 Å for the parallel pair.

2.2 Crystal Structure of the Molecular Helix

The title complex crystallizes in a centrosymmetric space group *P* $\bar{1}$, consequently the molecules occur as

Table 2 Selected Bond Lengths(Å) and Bond Angles(°)

Fe(1)-O(6)	1.910(3)	Fe(1)-O(2)	1.925(2)	Fe(1)-N(6)	2.172(3)
Fe(1)-O(5)	1.889(3)	Fe(1)-O(1)	1.922(3)	Fe(1)-N(5)	2.167(3)
Fe(1)-O(4)	1.921(3)	Fe(1)-N(2)	2.136(3)	Fe(1)-N(4)	2.179(3)
Fe(2)-O(3)	1.921(3)	Fe(2)-N(1)	2.122(3)	Fe(2)-N(3)	2.163(3)
O(6)-Fe(1)-O(4)	94.6(1)	O(4)-Fe(1)-O(2)	96.0(1)	O(4)-Fe(1)-N(2)	100.2(1)
O(6)-Fe(1)-N(6)	81.9(1)	O(2)-Fe(1)-N(6)	99.1(1)	O(6)-Fe(1)-N(4)	96.6(1)
O(2)-Fe(1)-N(4)	165.4(1)	N(6)-Fe(1)-N(4)	84.6(1)	O(6)-Fe(1)-O(2)	97.9(1)
O(6)-Fe(1)-N(2)	165.2(1)	O(2)-Fe(1)-N(2)	81.2(1)	O(4)-Fe(1)-N(6)	164.8(1)
N(2)-Fe(1)-N(6)	83.6(1)	O(4)-Fe(1)-N(4)	81.2(1)	N(2)-Fe(1)-N(4)	85.2(1)
O(5)-Fe(2)-O(1)	97.6(1)	O(5)-Fe(2)-N(1)	94.6(1)	O(1)-Fe(2)-N(1)	82.4(5)
O(3)-Fe(2)-N(5)	93.7(1)	N(1)-Fe(2)-N(5)	86.6(1)	O(3)-Fe(2)-N(3)	81.6(1)
N(1)-Fe(2)-N(3)	84.9(1)	O(5)-Fe(2)-O(3)	98.9(1)	O(3)-Fe(2)-O(1)	97.3(1)
O(3)-Fe(2)-N(1)	166.4(1)	O(5)-Fe(2)-N(5)	81.8(1)	O(1)-Fe(2)-N(5)	168.9(1)
O(5)-Fe(2)-N(3)	166.2(1)	O(1)-Fe(2)-N(3)	95.9(1)	N(5)-Fe(2)-N(3)	84.4(1)

racemic mixture of P and M configuration enantiomers, as shown in Fig. 2. Each iron center is bound to three ON binding units from three different ligands to attain distorted octahedral coordination geometry with the Fe...Fe separation of *ca.* 3.89Å. Each ligand loses two protons and coordinates to two metal centers as a bis(bidentate) ligand to complete the helical fashion. The Fe-O distance are in the range of 1.912(3) ~ 1.928(2)Å and the Fe-N distances are in the range of 2.139(3) ~ 2.175(3)Å, respectively. There are three sets of bond angles O-Fe-N in the ranges of 81.1(1)° ~ 82.6(1)°, 93.8(1)° ~ 100.1(1)° and 164.8(1)°

~ 168.9(1)°, respectively. The O-Fe-O and N-Fe-N are in the ranges of 94.8(1)° ~ 98.0(1)° and 83.6(1)° ~ 86.4(1)°, respectively. Bond distances of the side chain are all intermediate between formal single and double bonds, pointing to extensive electron delocalization over the entire moiety of each ligand. Coordination to the metal center forces interplanar twisting between the two naphthyl rings of each ligands. The dihedral angle is 85.2(3)° between the naphthyl rings I and II, *ca.* 86.1(4)° between the naphthyl rings III and IV, and 68.2(3)° between the naphthyl rings V and VI, respectively, where the naphthyl rings from I to VI are containing oxygen atoms O(1), O(2), O(3), O(4), O(5) and O(6), respectively. It is suggested that the π - π stacking interactions are considered to be important in stabilizing this complex.

It is also interesting to find that the naphthyl rings II and symmetry-related ring II A (symmetry code A: $1 - x, -y, -z$); the naphthyl rings IV and symmetry-related ring V B (symmetry code B: $-1 + x, -1 + y, z$), the naphthyl rings III and symmetry-related ring VI C (symmetry code c: $1 - x, -y, 1 - z$), connected each other to form a two-dimensional sheets with channels (Fig. 3). The dihedral angle for the stacked pairs is 0° (II/II A), 3.7° (III/VI) and 10.6° (IV/V), respectively. The shortest inter-planar atom...atom separation for the stacked pairs is 3.43Å (II/II A), 3.60Å (VI/V) and 3.51Å (III/VI) respectively. Three DMF molecules per formula unit are found

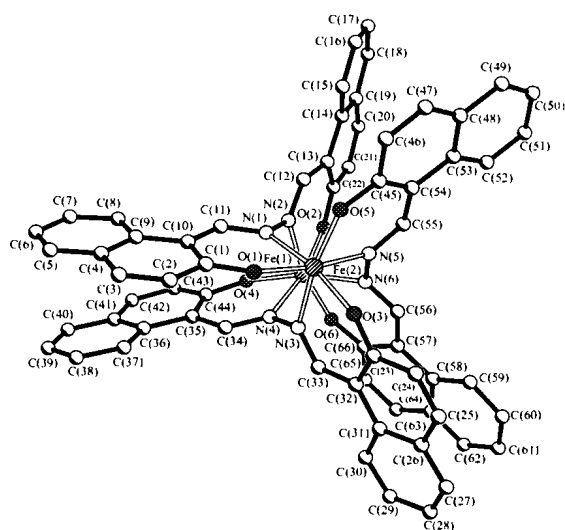


Fig. 2 Molecular structure of the title compound with the atom numbering scheme
Hydrogen atoms and solvent molecules are omitted for clarity

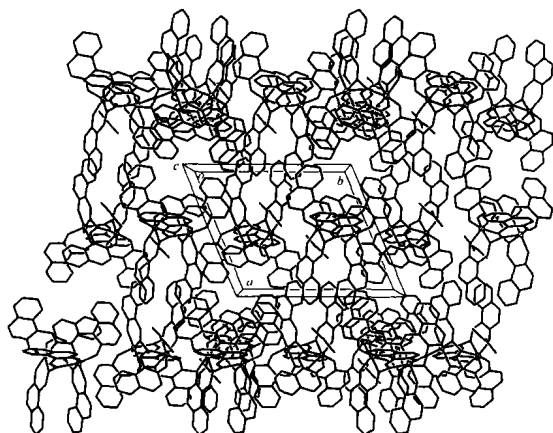


Fig. 3 Molecular packing along the *c*-axis showing the channelled structure

The guest molecules were omitted for clarity

to fill the channel. There are no obviously interactions between the guest and the two-dimensions sheets was found.

2.3 Thermogravimetric Analysis

The most important factor in seeking and developing new molecular-based porous materials is whether the frameworks of such materials are stable even after removal of guest molecules^[13]. As we know, many porous systems, upon removal of the included guest molecules, often undergo phase transitions to other more dense structures^[14,15]. To evaluate the mobility of the guests within the framework, we examined the as-synthesized crystals by thermogravimetric techniques (Fig. 4). In flowing nitrogen, a crystalline sample was heated at a constant rate of $5^{\circ}\text{C} \cdot \text{min}^{-1}$. A rapid weight loss of 14.3% was observed below 150°C corresponding to the liberation of all three DMF guests per formula unit (Calcd: 14.0%), and at the temperature

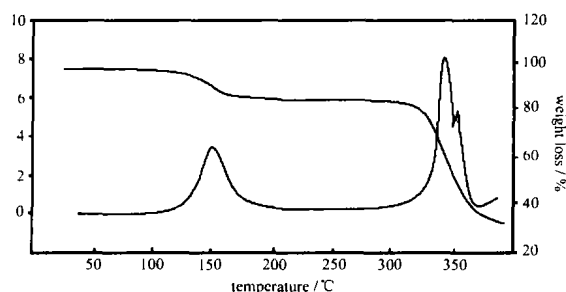


Fig. 4 EG and TGA for compound **1** from 25 to 400°C

range of $150 \sim 300^{\circ}\text{C}$, almost no weight loss was observed. Beyond this temperature, a weight loss step from 300 to 350°C was observed and attributed to decomposition of the framework. It is suggested that such a framework is retained in the absence of guest molecules at $150^{\circ} \sim 250^{\circ}$.

In conclusion, the present study shows the new example of 2D channelled structure assembled from triple helices. The assembly of helical units into a metal-organic porous open framework is interesting both in term of controlled aggregation of helices and porous materials. The absence of counter ions and the significant large internal void make these and related materials exciting new candidates for examination of their potential utilities in, for example, catalysis or separation processes. It is also worthy to note that although the energy of π - π interactions is only $2 \sim 20\text{kJ} \cdot \text{mol}^{-1}$, this kind of non-covalent bond has the potential to assemble smaller and simpler fragments into the desired cavities under favorable conditions, which is important in host-guest chemistry and has applications in chemistry, biology and material science.

Acknowledgements: We thank Mr. LIU Yong-Jiang in Nanjing University for collecting the crystal data.

References

- [1] (a) Lehn J. -M. *Supramolecular Chemistry: Concept and Perspectives*, VCH: Weinheim, **1995**;
- (b) Atwood J. L., Davies J. E. D., MacNicol D. D., Vögtle F., Lehn J. -M. Eds. *Comprehensive Supramolecular Chemistry*, Pergamon: Oxford, **1996**, Vol. **9**, p165 ~ 211, 213 and 282.
- [2] (a) Fujita M. *Chem. Soc. Rev.*, **1998**, **27**, 417;
- (b) Stang P. J., Olenyuk B. *Acc. Chem. Res.*, **1997**, **30**, 502;
- (c) Saalfrank R. W., Bernt I. *Curr. Opin Solid State Mater.*, **1998**, **3**, 407;
- (d) MacGillivray L. R., Atwood J. L. *Angew. Chem., Int. Ed.*, **1999**, **38**, 1018.
- [3] (a) Takeda N., Umemoto K., Yamaguchi K., Fujita M. *Nature (London)*, **1999**, **398**, 794;
- (b) Baxter P. N. W., Lehn J. -M., Rissanen K. *Chem.*

- Commun.*, **1997**, 1323;
(c) Baxter P. N. W., Hanan G. S., Lehn J. -M. *Chem. Commun.*, 1996, 2019.
- [4] (a) Piguet C., Bernardinelli G., Hopfgartner G. *Chem. Rev.*, **1997**, **97**, 2005;
(b) Constable E. C. *Polynuclear Transition Metal Helicates in Comprehensive Supramolecular Chemistry*, ed. Sauvage J. -P. Elsevier: Oxford, **1996**, Vol. **9**, p213 ~ 252.
- [5] (a) Hasenknopf B., Lehn J. -M., Boumediene N., Dupont-Gervais A., Dorselaer A. V., Kneisel B., Fenske D. *J. Am. Chem. Soc.*, **1997**, **119**, 10956;
(b) Hannon M. J., Painting C. L., Jackson A., Hamblin J., Errington W. *Chem. Commun.*, **1997**, 1807.
- [6] (a) Fang C. J., Duan C. Y., He C., Meng Q. J. *Chem. Commun.*, **2000**, 1187;
(b) He C., Duan C. Y., Fang C. J., Meng Q. J. *J. Chem. Soc. Dalton Trans.*, **2000**, 2419;
(c) Fang C. J., Duan C. Y., Mo H., He C., Meng Q. J., Liu Y. J., Mei Y. H., Wang Z. M. *Organometallics*, **2001**, **20**, 2525.
- [7] (a) Albrecht M., Kotila S. *Angew. Chem. Int. Ed. Engl.*, **1995**, **34**, 2134;
(b) Xu J., Parac T. N., Raymond K. N. *Angew. Chem. Int. Ed. Engl.*, **1999**, **38**, 2878;
(c) Kersting B., Meyer M., Powers R. E., Raymond K. N. *J. Am. Chem. Soc.*, **1996**, **118**, 7221.
- [8] Bowyer P. K., Porter K. A., Rae A. D., Willis A. C., Wild S. B. *Chem. Commun.*, **1998**, 1153.
- [9] (a) Hannon M. J., Painting C. L., Alcock N. W. *Chem. Commun.*, **1999**, 2023;
(b) Hannon M. J., Bunce S., Clarke A. J., Alcock N. W. *Angew. Chem. Int. Ed. Engl.*, **1999**, **38**, 1277.
- [10] Ziessel R., Harriman A., El-Ghayoury A., Douce L., Leize E., Nierengarten H., Dorselaer A. V. *New. J. Chem.*, **2000**, **24**, 729.
- [11] *SMART and SAINT. Area Detector Control and Integration Software*, Siemens Analytical X-Ray Systems, Inc., Madison, Wisconsin, USA, **1996**.
- [12] Sheldrick G. M. *SHELXTL V5.1 Software Reference Manual*, Bruker AXS, Inc., Madison, Wisconsin, USA. **1997**.
- [13] (a) Gardner G. B., Kiang Y. -H., Lee S., Asgaonkar A., Venkataraman D. *J. Am. Chem. Soc.*, **1996**, **118**, 6946;
(b) Kitagawa S., Kondo M. *Bull. Chem. Soc. Jpn.*, **1998**, **71**, 1739.
- [14] Wang X., Simard M., Wuest J. D. *J. Am. Soc. Chem.*, **1994**, **116**, 12119.
- [15] (a) Hoskins B. F., Robson R. *J. Am. Soc. Chem.*, **1990**, **112**, 1546;
(b) Abrahams B. F., Hoskins B. F., Michail D. M., Robson R. *Nature*, **1994**, **369**, 727.